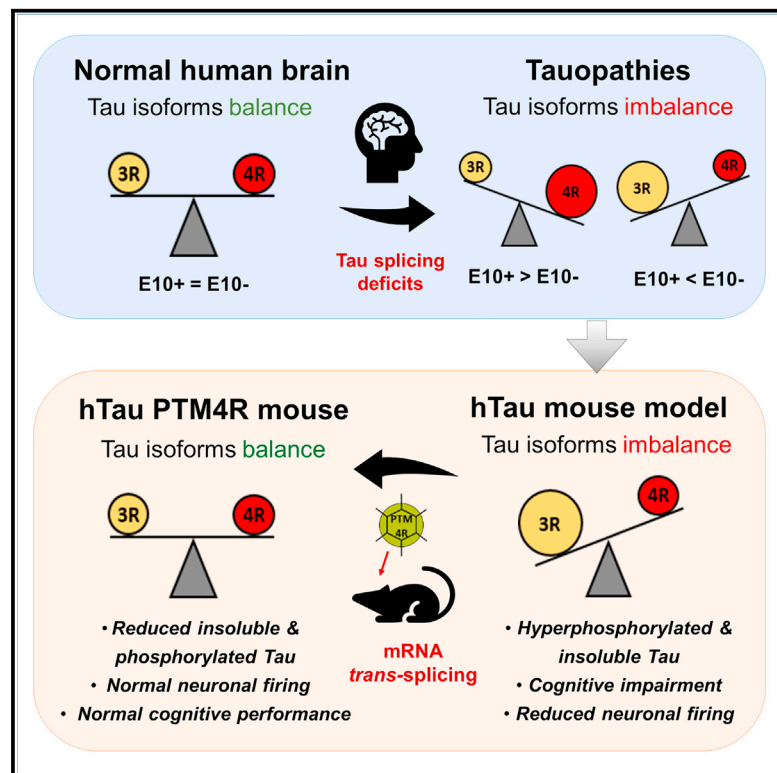


Modulation of Tau Isoforms Imbalance Precludes Tau Pathology and Cognitive Decline in a Mouse Model of Tauopathy

Graphical Abstract



Authors

Sonia Lorena Espíndola, Ana Damianich, Rodrigo Javier Alvarez, ..., Juan Esteban Ferrario, Jean-Marc Gallo, María Elena Avale

Correspondence

elena.avale@conicet.gov.ar

In Brief

Tau isoform imbalances in humans lead to neurological disorders. Espíndola et al. show that *in vivo* reprogramming of tau mRNA by *trans*-splicing in adult transgenic mice corrects tau isoform imbalance, yielding reduced pathological markers and preventing the loss of key functions such as neuronal activity and cognitive performance.

Highlights

- Htau mice show cognitive deficits and tau pathology with reduced PFC activity
- *In vivo trans*-splicing yields long-term modulation of tau 3R/4R isoform ratio
- Early balance of tau isoforms in the PFC reduces tau pathology in aged htau mice
- Tau reprogramming prevents cognitive impairment and deficits in neuronal firing



Modulation of Tau Isoforms Imbalance Precludes Tau Pathology and Cognitive Decline in a Mouse Model of Tauopathy

Sonia Lorena Espíndola,¹ Ana Damianich,¹ Rodrigo Javier Alvarez,^{3,4,6} Manuela Sartor,^{1,6} Juan Emilio Belforte,^{3,4} Juan Esteban Ferrario,² Jean-Marc Gallo,⁵ and María Elena Avale^{1,7,*}

¹Instituto de Investigaciones en Ingeniería Genética y Biología Molecular, Consejo Nacional de Investigaciones Científicas y Técnicas (INGEBI-CONICET), Buenos Aires, Argentina

²Instituto de Investigaciones Farmacológicas (ININFA-CONICET-UBA), Buenos Aires, Argentina

³Universidad de Buenos Aires, Facultad de Medicina, Departamento de Fisiología, Buenos Aires, Argentina

⁴Instituto de Fisiología y Biofísica “Bernardo Houssay” (IFIBIO-Houssay-CONICET), Buenos Aires, Argentina

⁵Maurice Wohl Clinical Neuroscience Institute, Institute of Psychiatry, Psychology and Neuroscience, King’s College London, London, UK

⁶These authors contributed equally

⁷Lead Contact

*Correspondence: elena.avale@conicet.gov.ar
<https://doi.org/10.1016/j.celrep.2018.03.079>

SUMMARY

The microtubule-associated protein tau regulates myriad neuronal functions, such as microtubule dynamics, axonal transport and neurite outgrowth. Tauopathies are neurodegenerative disorders characterized by the abnormal metabolism of tau, which accumulates as insoluble neuronal deposits. The adult human brain contains equal amounts of tau isoforms with three (3R) or four (4R) repeats of microtubule-binding domains, derived from the alternative splicing of exon 10 (E10) in the tau transcript. Several tauopathies are associated with imbalances of tau isoforms, due to splicing deficits. Here, we used a *trans*-splicing strategy to shift the inclusion of E10 in a mouse model of tauopathy that produces abnormal excess of 3R tau. Modulating the 3R/4R ratio in the prefrontal cortex led to a significant reduction of pathological tau accumulation concomitant with improvement of neuronal firing and reduction of cognitive impairments. Our results suggest promising potential for the use of RNA reprogramming in human neurodegenerative diseases.

INTRODUCTION

Tau is a microtubule-associated protein, enriched in neuronal axons, that regulates neurite outgrowth and axonal transport, among other functions (Arendt et al., 2016; Medina et al., 2016; Morris et al., 2011). Under pathological conditions, such as gene mutations, failures in post-translational processing or clearance (reviewed in Bodea et al., 2016), hyperphosphorylated insoluble tau accumulates in the neuronal soma. These tau deposits are the hallmark of several diseases, referred to as tauopathies, which include Alzheimer’s disease and frontotem-

poral dementia with parkinsonism linked to chromosome 17 (FTDP-17) (reviewed in Spillantini and Goedert, 2013).

Human tau is encoded by the *MAPT* gene, comprising 16 exons that produce six different tau isoforms in the adult brain, by alternative splicing of exons 2, 3, and 10 (Andreadis, 2005). Alternative splicing of exon 10 (E10) gives rise to tau isoforms with three (3R) or four (4R) microtubule-binding repeats (Andreadis et al., 1992; Goedert et al., 1989), found in equal amounts in the normal adult human brain. Imbalances in tau 3R/4R ratio are known as a disease-causative phenomenon, initially based on genetic evidence from patients carrying mutations affecting E10 splicing (Hutton et al., 1998; Spillantini et al., 1998). So far, more than 50 mutations have been found in the *MAPT* gene (Qian and Liu, 2014; Spillantini and Goedert, 2013), with about one-third of them affecting E10 splicing and consequently the normal 3R/4R balance (Niblock and Gallo, 2012). The majority of those mutations favor E10 inclusion, leading to 4R increase (Spillantini and Goedert, 2013), but mutations yielding 3R excess were also linked with disease (Stanford et al., 2003), suggesting that tau isoform imbalance is detrimental regardless of whether the ratio shifts toward 3R or 4R (reviewed in Andreadis, 2012). Although their etiology is known, no treatment has become available for those tauopathies; yet, early correction of aberrant E10 splicing arises as a potential therapeutic strategy to stop the onset of disease.

We previously validated the spliceosome-mediated RNA *trans*-splicing (Rodríguez-Martin et al., 2005) as a procedure to modulate endogenous tau E10 inclusion in the mouse brain (Avale et al., 2013) and in human neurons in culture (Lacovich et al., 2017). Here, we used this strategy to investigate whether modulation of relative content in tau isoforms prevents the development of pathological phenotypes in the htau mouse (Andorfer et al., 2003), a validated model of tauopathy. Htau mice carry a full-length human *MAPT* gene that produces the six human tau isoforms in the adult brain, where production of 3R isoforms are favored over 4R. It was suggested that such 3R > 4R content might underlie tau pathology and the associated phenotypes observed in aged htau mice, such as tau hyperphosphorylation



(Andorfer et al., 2003) and cognitive deficits (Polydoro et al., 2009). To test this hypothesis, we used *trans*-splicing to enhance E10 inclusion into the medial prefrontal cortex of adult htau mice. *Trans*-splicing reduced the contents of pathological tau in htau mice, which showed normal electrophysiological and behavioral performance, suggesting that early modulation of 3R/4R tau isoforms ratio has a beneficial effect over the tauopathy phenotypes in this model.

RESULTS

Reprogramming of 3R to 4R Tau Isoforms in the Prefrontal Cortex of Htau Mice

Tau pathology was reported both in the cortex and hippocampus of htau mice (Andorfer et al., 2003; Polydoro et al., 2009). Yet we found the most prominent accumulation of pathological tau in the medial prefrontal cortex (mPFC) (Figure S1). Moreover, the phenotypes we observed in this model are consistent with prefrontal dysfunction, so we selected the mPFC to modulate the 3R/4R ratio and analyze the potential functional rescue.

To promote E10 inclusion into endogenous tau transcripts, we used a pre-*trans*-splicing molecule (PTM), delivered by a lentiviral vector, (LV)-PTM4R (Figure 1A), as previously described (Avale et al., 2013). The *trans*-splicing reaction yields a chimeric RNA containing E10+, which codes for a 4R tau isoform. Control mice were injected with an LV carrying the same construct but lacking the *trans*-splicing domain (LV-PTM4R- Δ TSD; Figure 1B). LV-PTMs were injected at 2–3 months of age, before the onset of pathological tau accumulation. Behavioral, electrophysiological, and biochemical analyses were performed in 10- to 12-month-old mice (Figure 1C).

Endpoint RT-PCR (Figure 1D) was performed to visualize tau mRNA isoforms using primers spanning exons 9–13 of the tau transcript. As previously reported (Avale et al., 2013), htau mice produce very low amounts of E10+, which increased after PTM4R administration (htau-PTM4R). To perform a quantitative analysis of tau mRNA isoforms, real-time qPCR was performed after laser-captured microdissection of the mPFC co-injected with LV-PTMs and a fluorescent reporter (LV-GFP; Figure 1E). Htau-control mice showed excess of E10– over E10+ tau mRNA, yielding E10+/E10– ratio of 0.5 (Figures 1F and S1D). Conversely, htau-PTM4R showed an increase in E10+ concomitant with a decrease in E10 (Figure S1D), leading to a ratio of \sim 0.8 (Figure 1F). As expected, the injection of *trans*-splicing molecules did not alter total tau mRNA amounts (Figure 1G), both htau-PTM4R and htau-control-injected mice showed similar total tau levels as non-injected (NI) htau mice.

Western blot analyses using 3R and 4R specific antibodies showed that htau-control mice display 2-fold 3R tau protein over 4R tau, while htau-PTM4R mice showed similar 3R and 4R tau protein levels in the PFC (Figures 1H and S2A). As expected, wild-type (WT) mice evidenced almost all 4R content, with very low amounts of 3R tau. Total tau levels were similar between htau-control, htau-PTM4R, and htau non-injected groups (Figure 1I), which in turn show increased total tau levels compared with the WT group (Figures 1I and S2A), consistent with previous reports (Andorfer et al., 2003; Duff et al., 2000).

The control vector (LV-PTM4R- Δ TSD) did not alter tau contents in htau mice (Figure 1I) or in WT mice (Figure S2B). The injection of LV-PTM4R drove E10 inclusion in the mPFC and adjacent M2 cortex, but not in other brain areas where the 3R > 4R imbalance was observed in htau-PTM4R mice (Figure S2C). Together, these data highlight the efficiency and specificity achieved with the *trans*-splicing strategy to locally modulate 3R/4R ratio into the adult htau brain.

Reduction of Insoluble and Hyperphosphorylated Tau in Htau-PTM4R Mice

Accumulation of insoluble hyperphosphorylated tau is a hallmark of human tau pathology, recapitulated in htau mice (Andorfer et al., 2003; Castillo-Carranza et al., 2015; Duff et al., 2000; Noble et al., 2009). To determine whether early modulation of the 3R/4R ratio could prevent tau pathology, we analyzed the accumulation of hyperphosphorylated tau in brain sections spanning the mPFC of aged mice (>12 months) that had been injected at 3 months with either LV-PTM4R (htau-PTM4R) or LV-PTM4R- Δ TSD vector (htau-control). Htau-control mice showed strong phospho-tau labeling along the PFC (Figures 2A–2D), detected by two different specific antibodies recognizing tau phosphorylated at Ser 202 (CP13; Figure 2A) or at Thr231/Ser235 (AT-180; Figure 2C). Quantitative analyses revealed that in the htau-PTM4R group, the number of positive cells stained with both antibodies was significantly reduced compared with htau controls (Figures 2B and 2D).

Total amounts of hyperphosphorylated tau were also measured by western blotting in PFC homogenates of aged htau-PTM4R, htau-control, and WT mice (Figures 2E and 2F). A significant increase was observed in htau-control mice compared with WT mice, either at Ser 202 (Figures 2E and S2D) or at Thr231/Ser235 (Figure 2F), while htau-PTM4R mice showed values similar to WT mice (Figures 2E, 2F, and S2D).

We also quantified tau protein levels in soluble and insoluble protein fractions obtained from PFC homogenates by sarkosyl fractionation. Htau-control mice showed high amounts of insoluble tau (Figure 2G), yielding a 4-fold increase in the insoluble/soluble ratio compared with WT (Figure 2H), while htau-PTM4R mice showed a significant reduction in the insoluble tau fraction (Figure 2G), leading to a soluble/insoluble tau ratio similar to control WT mice (Figure 2H). Taken together, these results indicate that early local modulation of tau 3R/4R balance prevents the accumulation of insoluble/hyperphosphorylated tau in the PFC of aged htau mice.

Electrophysiological and Behavioral Phenotypes of Htau-PTM4R Mice

To assess whether a functional recovery could be achieved because of tau isoform modulation in the PFC of htau mice, we characterized the neuronal firing in aged mice, recording the electrophysiological activity of putative pyramidal neurons. Three tetrodes were placed in the mPFC of anesthetized mice, either htau-control, htau-PTM4R, or WT group, and extracellular unit activity was analyzed according to published criteria (de Almeida et al., 2013). Normal neuronal activity was disrupted in the htau-control group, which displayed a significant decrease in mean firing rate compared with age-matched controls (Figures

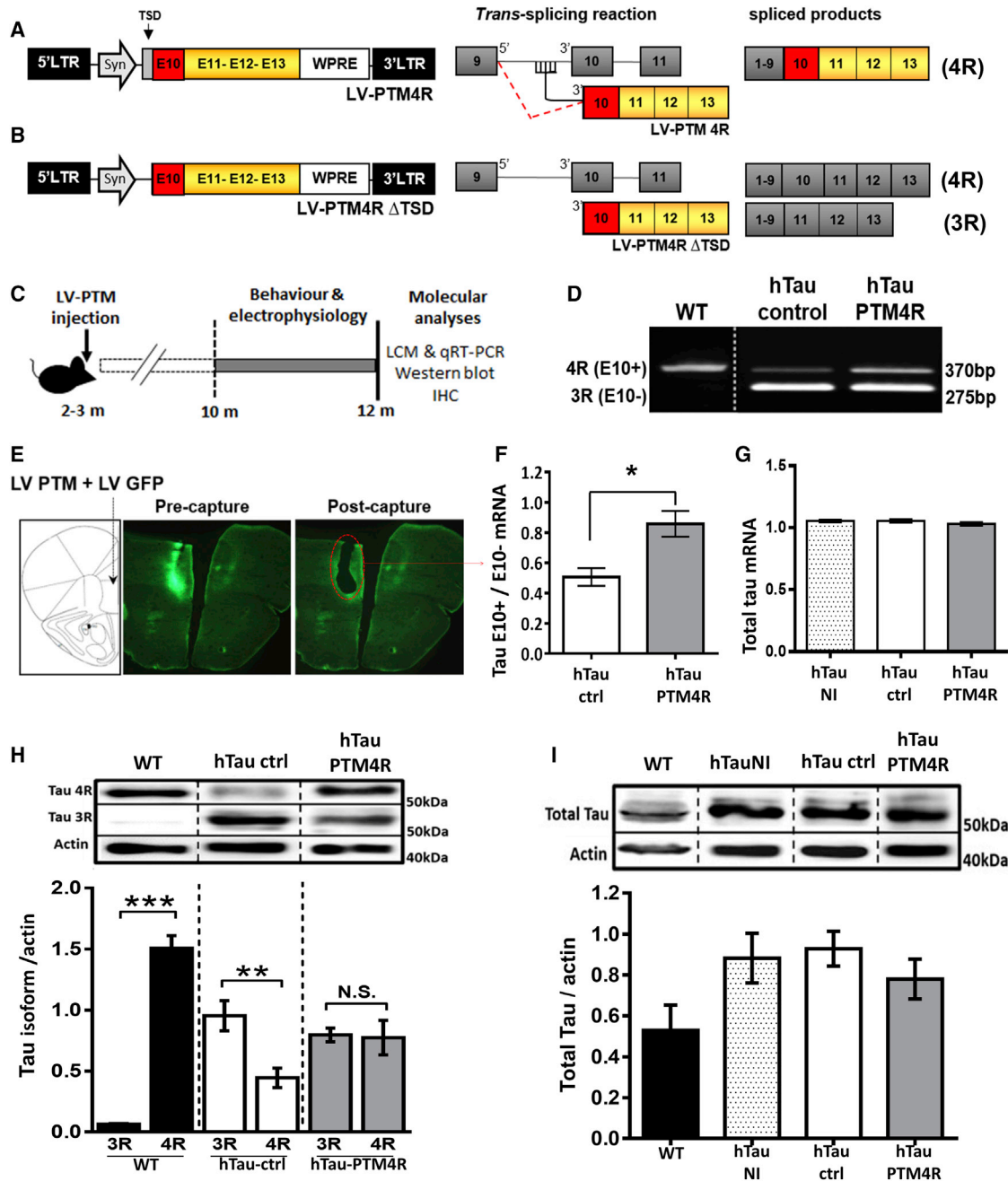


Figure 1. Local Reprogramming of 3R to 4R Tau Isoforms in the Prefrontal Cortex of Htau Mice

(A and B) Map of lentiviral vectors. (A) LV-PTM4R used for *trans*-splicing and the expected chimeric transcript containing E10. (B) Lentiviral vector LV-PTM4R Δ TSD used for control mice.

(C) Time course of the experiments performed in the study.

(D) Analysis of tau isoforms by endpoint RT-PCR with primers spanning E9 and E13.

(E) Laser-capture microdissection of the mPFC of htau mice co-injected with LV-PTM and an LV carrying GFP.

(F) Relative content of tau isoforms determined by RT-qPCR with specific primers for 3R (E10 $-$) and 4R (E10 $+$). Data are expressed as the isoform ratio; mean \pm SEM; * p < 0.05, two-tailed t test; n = 4 per group.

(G) Total tau mRNA, showing no differences among treatments.

(H and I) Western blot detection of tau protein contents in PFC homogenates. (H) Tau isoforms 3R and 4R contents and (I) total tau protein, related to actin loading control. Mean \pm SEM; ** p < 0.01 and *** p < 0.001, two-tailed t test (WT = 3, htau-control = 4, and htau-PTM4R = 5, htau Ni = 3). Full blots are shown in [Figure S2A](#).

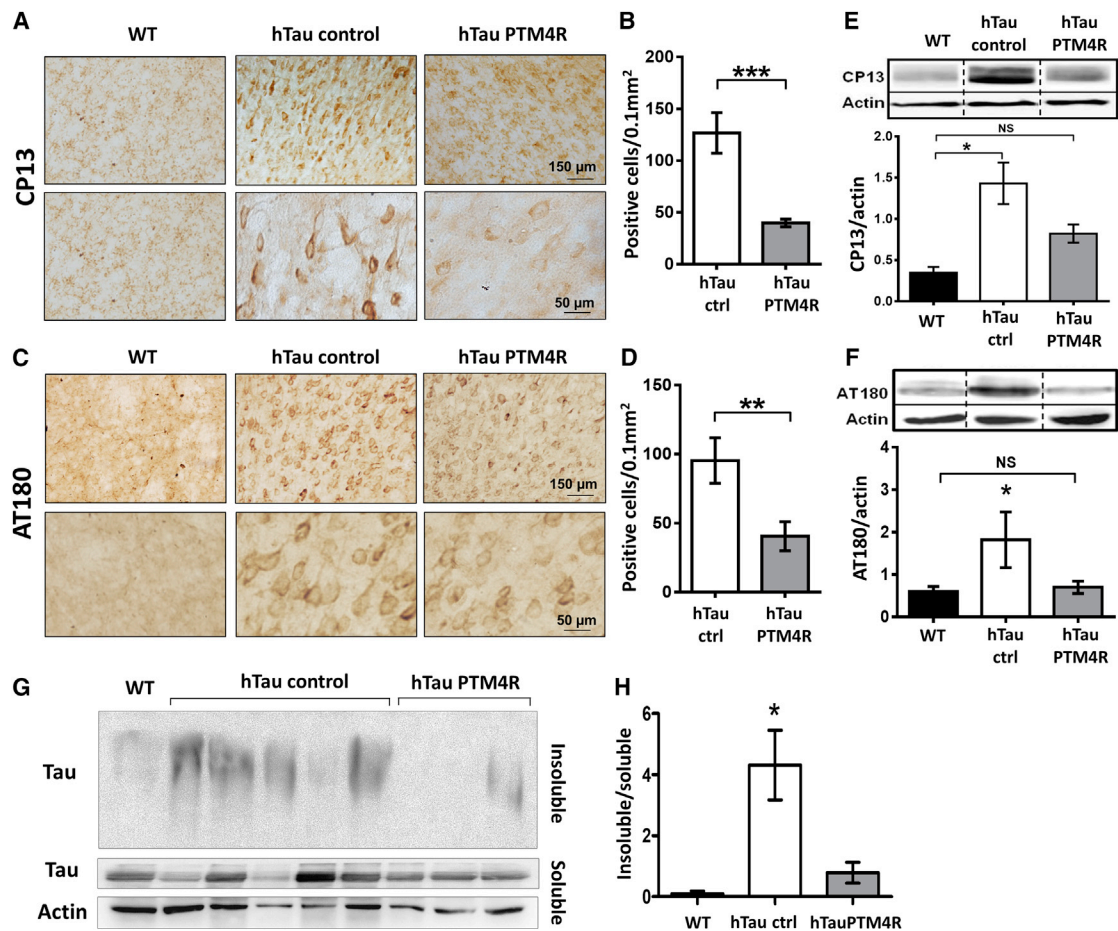


Figure 2. Hyperphosphorylated and Insoluble Tau Contents in the PFC

(A–D) Hyperphosphorylated tau detected by immunohistochemistry using CP13 (S202) (A and B) and AT180 (T231/S235; C and D) antibodies in coronal sections spanning the mPFC. (B and D) Quantification of positive cells in htai-control and htai-PTM4R. CP13, n = 3 per group; AT180, n = 4 per group; two to four sections per mouse; mean ± SEM; **p < 0.01 and ***p < 0.001, two-tailed t test.

(E and F) Hyperphosphorylated tau protein contents determined by western blot in PFC homogenates using CP13 (E) in WT (n = 4), htai-control (n = 6), and htai-PTM4R (n = 6) or (F) AT180: WT (n = 3), htai-control (n = 4), and htai-PTM4R (n = 7). Mean ± SEM; *p < 0.05, one-way ANOVA followed by Tukey's post hoc test. Full blots are shown in Figure S2D.

(G and H) Sarkosyl insolubility assay. Soluble and insoluble fractions obtained from PFC homogenates were immunoblotted (G) to quantify total tau in each fraction (H). WT, n = 2; htai-control, n = 4; htai-PTM4R, n = 3; mean ± SEM; *p < 0.05, one-way ANOVA followed by Tukey's post hoc test.

3A, 3B, S3C, and S3D). Remarkably, balancing 3R/4R tau isoforms in htai-PTM4R mice resulted in a recovery of neuronal activity, with a mean firing rate similar to the observed WT mice (Figures 3B and S3C). Furthermore, the population of active neurons firing over 4 Hz was decreased in htai-control mice compared with WT (WT, 21.4%; htai, 7.7%; chi-square p = 0.034) and was recovered in hTau-PTM4R (WT, 21.4%; htai-PTM4R, 25.5%; chi-square p = 0.59) (Figure 3B).

We next analyzed cognitive performance in the novel object recognition (NOR) test, a task known to rely on mPFC integrity (Morici et al., 2015), which is severely impaired in htai mice (Castillo-Carranza et al., 2014; Polydoro et al., 2009). As previously reported, aged htai-control mice exhibited poor recognition performance, showing a discrimination index of 50%, compared with the 80% observed in the WT group (Figure 3C). Interestingly,

htai-PTM4R mice showed similar performance as WT to discriminate the novel object (Figure 3C), demonstrating full recovery on this task. The time spent in exploration was similar between groups (Figure 3D). Yet an open-field analysis revealed a small increase in total locomotion in htai-control mice compared with WT (Figure 3E), with more activity in the center of the arena (Figure 3F). However, these phenotypes were only partially rescued in the htai-PTM4R group, showing no differences from WT and htai-control groups. On the other hand, when tested in the elevated plus maze, htai-control mice displayed about 50% of entries into open arms (Figures 3G and 3H), suggesting no preference for protected arms, while htai-PTM4R mice showed 33% entries, similar to WT mice. However, no statistically significant differences were observed between groups on this task. Moreover, in our hands the htai model did not

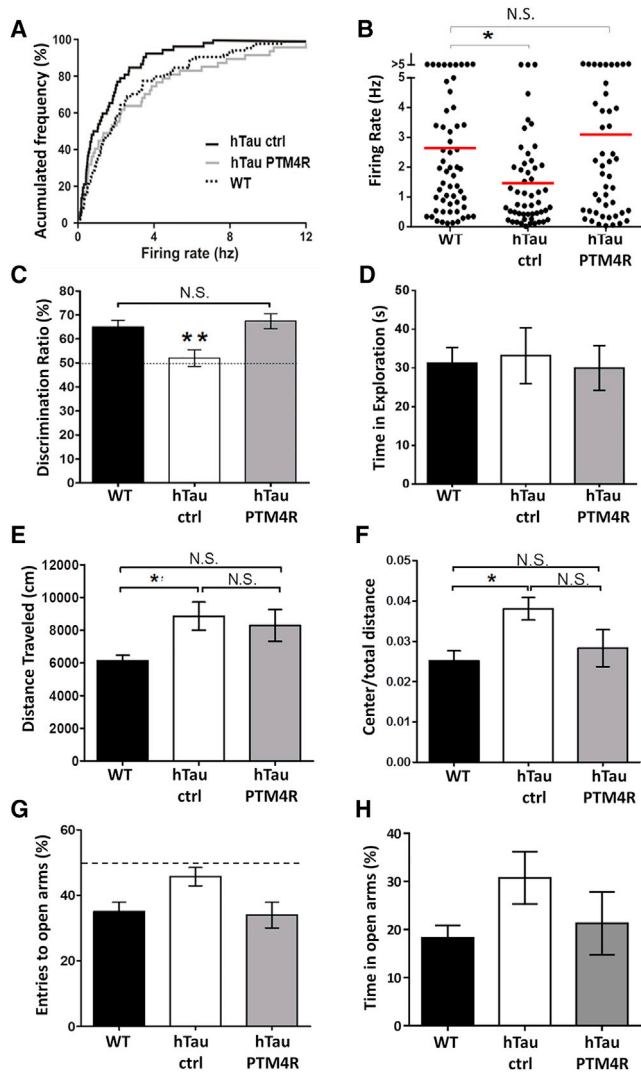


Figure 3. Functional Recovery in Htau-PTM4R Mice

(A and B) Electrophysiological activity in the PFC.
 (A) Accumulated firing frequency of putative pyramidal neurons during 30 min in WT (n = 4), htau-control (n = 3), and htau-PTM4R (n = 3) mice.
 (B) Firing rate of all recorded units for each experimental group. Each dot represents the mean firing rate of a putative pyramidal unit recorded in the PFC during 30 min. Red bars indicate mean firing rate of the entire population of single units recorded per group; htau-ctrl was significant different ($p < 0.05$ versus WT, Kruskal-Wallis $H_{2,183} = 6.8$, $p = 0.0329$). WT, n = 84; htau control, n = 52; and htau-PTM4R, n = 47 neurons from four, three, and three mice, respectively.
 (C and D) Novel object recognition task. (C) Discrimination ratio of the novel object and (D) total time exploring objects (WT, n = 16; htau-control, n = 14; htau-PTM4R, n = 13). Individual data are shown in Figures S3D and S3E.
 (E and F) Spontaneous locomotion in the open field. (E) Total distance traveled and (F) activity ratio in the center of the arena recorded during 30 min. WT, n = 11; htau-control, n = 8; and htau-PTM4R, n = 4. Data in (C)–(F) are mean \pm SEM; * $p < 0.05$ and ** $p < 0.01$, one-way ANOVA followed by Tukey's test. Individual data points are shown in Figure S3C.
 (G and H) Elevated plus maze task. (G) Percentage of entries into open arms and (H) time spent in open arms. Mean \pm SEM, n = 4. No significant differences among groups (Kruskal-Wallis non-parametric test). Individual data are shown in Figure S3F.

show impairments in spatial memory assessed in the Morris water maze test; both control and htau-PTM4R mice performed similarly to WT mice (Figures S3A and S3B). Together, electrophysiological and behavioral analyses indicate that the local early modulation of tau isoforms in htau mice prevents impairments in PFC functionality and restores normal performance in the NOR task.

DISCUSSION

In this study we show that modulation of 3R/4R tau isoform balance in the prefrontal cortex precludes tau pathology and related phenotypes in the htau mouse model of tauopathy.

The use of mouse models to analyze tau isoform imbalance is challenging, because 4R is the only isoform present in the WT adult mouse brain. By contrast, the htau model bears a full-length normal human *MAPT* transgene that, despite the lack of mutations, favors E10 exclusion and produces an excess of 3R isoform. This might be due to the lack of specific splicing regulatory elements in the mouse neurons (or a different combination of splicing factors), which impairs the correct processing of the human tau transcript. Thus, compared with either the adult human brain expressing both isoforms in an equimolar ratio or with WT adult mouse brain, which expresses 4R tau only, the htau brain has an aberrant content of tau isoforms that correlates with tau pathology (Andorfer et al., 2003). Moreover, tau pathology is not likely to be due to tau overexpression in this model, as the same transgene in a WT background does not recapitulate tauopathy (Duff et al., 2000), suggesting that endogenous murine 4R tau might balance the excess of human 3R tau. These features make the htau model particularly interesting to test *in vivo* strategies that modulate E10 splicing and assess the phenotypic consequences of such modulation.

We have demonstrated herein that by increasing E10 inclusion, we reached a balanced 3R/4R ratio in the mPFC of htau-PTM4R mice, which prevents the pathological phenotypes observed under 3R excess in htau-control mice. It is noteworthy that *trans*-splicing strategy reduces tau pathology without changes in the total amount of tau protein compared with control htau, and creating a ~ 1.0 3R/4R ratio of human tau in adult mice is not detrimental. Indeed, in our conditions, the increase of the 4R isoform by means of the *trans*-splicing strategy did not induce tau pathology; instead, consistent rescue was observed in histological, functional, and behavioral analyses. Strikingly, enhancing 4R isoform by intraventricular ASO treatment was reported to induce tau pathology and seizures in young htau mice (Schoch et al., 2016). However, that study was performed at 4 months of age, before the onset of the phenotypes we and others analyzed in the htau model (Andorfer et al., 2003; Castillo-Carranza et al., 2015; Polydoro et al., 2009). On the other hand, ASO intracerebroventricular (i.c.v.) administration likely drives global 4R increase in the whole brain, which clearly differs from our strategy that locally targets a specific affected brain area. Our present results, in context with previous reports using this model, suggest that the long-term 3R > 4R imbalance might underlie tau pathology, particularly prefrontal dysfunction, in aged htau mice, which can be prevented by balancing the 3R/4R ratio at an early stage.

We have shown here that *trans*-splicing reprogramming of the endogenous tau transcript *in vivo* is a suitable strategy to achieve a phenotypic recovery. Our previous work (Lacovich et al., 2017) highlights the feasibility of this strategy to modulate tau isoform balance in human neurons, independent of the predominant isoform. Furthermore, RNA reprogramming can also correct missense mutations inside E10 (Rodriguez-Martin et al., 2009), without changing the total levels of tau protein. In this context, tau RNA reprogramming by *trans*-splicing arises as a versatile gene therapy approach with promising perspectives for human tauopathies. Further studies would be needed to optimize treatment conditions that ensure the most efficient therapeutics effects.

EXPERIMENTAL PROCEDURES

Mice

All animal procedures were designed in accordance with the NIH Guidelines for the Care and Use of Laboratory Animals, and protocols were approved by the Institutional Committee of INGEBI-CONICET (protocol number 005/2016) and FCEyN, University of Buenos Aires. Mice were housed under a 12 hr dark/light cycle with *ad libitum* access to food and water. Htau transgenic mice were obtained from Jackson Laboratories (stock number 005491) and bred to obtain htau and WT colonies. All mice were genotyped as previously described (Andorfer et al., 2003). Male adult mice were used to conduct all the experiments described in this study.

LVs

Tau PTMs were delivered into LVs, prepared as detailed previously (Avale et al., 2013) and in Supplemental Experimental Procedures.

Stereotaxic Injections

Male mice aged 8–10 weeks (weight 25–30 g) were bilaterally injected with 2 μ L of lentiviral suspension (0.6×10^7 TU/mL) into the PFC at the following coordinates (Paxinos and Franklin, 2011): anteroposterior, +2.5 mm; lateral, \pm 0.5 mm; and dorsoventral, -2.5 and -1.5 mm, measured from the bregma. Surgery was performed under the protocol detailed in Supplemental Experimental Procedures.

Laser-Capture Microdissection

Fluorescent areas were cut out of a series of eight to ten sections using the ArcturusXT laser-capture microdissection system (Thermo Fisher Scientific) by infrared (IR) laser energy combined with a UV cutting laser (Supplemental Experimental Procedures). Total RNA was isolated from the collected tissue (0.5 – 1 mm³), yielded 0.5 – 1 μ g RNA per sample.

Detection of Tau mRNA Isoforms

Total RNA was extracted using the RNeasy Lipid Tissue Kit (QIAGEN) or, in laser-capture microdissection (LCM)-dissected tissue, with the PicoPure RNA extraction Kit (Thermo Fisher Scientific). Reverse transcription was performed using TaqMan RT (Applied Biosystems) with 0.5 μ g of RNA and an equimolar ratio of oligo(dT) and random hexamers. Endpoint PCR was performed with primers spanning exons 9–13, as previously described (Avale et al., 2013). Human 4R, 3R, and total tau mRNA isoforms were detected using real-time PCR with specific pairs of primers per each isoform either spanning E9–E10 or E9/11–E11, respectively, or for all human tau isoforms spanning at E7–E8 (Supplemental Experimental Procedures).

Immunohistochemistry

Phosphorylated tau was detected on free-floating coronal sections (40 μ m) with either CP13 (1:100) or AT180 (1:500) (Thermo Fisher Scientific) monoclonal antibodies and developed with 3,3'-diaminobenzidine (DAB) (Sigma-Aldrich). Positive cells were quantified in the PFC between $+1.54$ and $+2.5$ mm from bregma.

Protein Extraction and Western Blotting

PFC homogenates were separated on 12% SDS-polyacrylamide gels, transferred, and blotted using antibodies directed against 3R tau (1:2,000 anti-tau 3-repeat isoform RD3; mouse monoclonal; Millipore), 4R tau (1:1,000 anti-tau 4-repeat isoform RD4; mouse monoclonal; Millipore), total tau (1:10,000 rabbit polyclonal; Dako), phospho-Ser202 (CP13 monoclonal, 1:300), AT-180 (1:1,000; Thermo Fisher Scientific), or mouse β -actin (mouse monoclonal, 1:10,000; Abcam). See details in Supplemental Experimental Procedures.

Sarkosyl Insolubility Assay

Fractionation of soluble and insoluble proteins was performed as previously described (Noble et al., 2009; Andorfer et al., 2003). Briefly, brains were homogenized, incubated with 1% sarkosyl reagent (Sigma-Aldrich), and ultracentrifuged to obtain soluble (supernatant) and insoluble (pellet) fractions (Supplemental Experimental Procedures). Total tau was detected on each fraction by western blot using total tau (1:10,000, rabbit polyclonal; Dako).

Electrophysiological Recordings

In vivo electrophysiological experiments we conducted as described previously (de Almeida et al., 2013). See Supplemental Experimental Procedures.

Behavioral Tests

All mice tested were sibling cohorts of males aged 10–12 months. Experiments were performed between 13:00 and 17:00 under dim illumination, in a separated behavioral room, where mice were transferred in advance. Behavioral experiments were analyzed by double-blinded operators.

Open Field

Activity boxes (Med Associates) were used to assess horizontal activity and trajectories, as previously described (Avale et al., 2004). See details in Supplemental Experimental Procedures.

Elevated Plus Maze

This test was performed as described previously (Avale et al., 2004). See details in Supplemental Experimental Procedures.

Novel Object Recognition

The protocol was performed similarly to that previously described (Polydoro et al., 2009), with minor modifications following a well-described methodological procedure (Leger et al., 2013). Briefly, in the training phase mice were allowed to explore identical objects for 10 min, and 5 hr later, mice were tested for 5 min in the same chamber with a familiar and a novel object. Discrimination index was calculated as the time spent exploring the novel object divided by the total time spent exploring both objects (familiar and novel). See details in Supplemental Experimental Procedures.

Statistical Analyses

Data were analyzed using GraphPad Prism. When normal distribution was assumed, the three experimental groups were analyzed using one-way ANOVA, followed by Tukey's test. When indicated, paired comparisons were done using two-tailed Student's *t* test. When normal distribution could not be assumed, the Kruskal-Wallis non-parametric test was used to compare groups.

SUPPLEMENTAL INFORMATION

Supplemental Information includes Supplemental Experimental Procedures and three figures and can be found with this article online at <https://doi.org/10.1016/j.celrep.2018.03.079>.

ACKNOWLEDGMENTS

This work was supported by the Argentinean National Research Council (CONICET) and the Ministry of Science (MINCYT; grant PICT2013-1109 to M.E.A. and grant PICT 2014-0459 to J.E.B.); the International Brain Research Organization (IBRO; to M.E.A. and J.E.F.), the International Society for Neurochemistry (grant ISN-CAEN 2015 to M.E.A.), and Foundation HDLorena. We thank Marcelo Rubinstein and Belen Elgoyhen for thoughtful advice and access to animal facilities and Tomas Falzone for helpful discussion.

AUTHOR CONTRIBUTIONS

S.L.E., A.D., R.J.A., and M.S. conducted experiments and analyzed data. J.E.B. and J.E.F. supervised experiments and analyzed data. J.-M.G. contributed materials and expertise. M.E.A. designed the project, supervised experiments, and wrote the paper.

DECLARATION OF INTERESTS

The authors declare no competing interests.

Received: August 11, 2017

Revised: February 7, 2018

Accepted: March 16, 2018

Published: April 17, 2018

REFERENCES

- Andorfer, C., Kress, Y., Espinoza, M., de Silva, R., Tucker, K.L., Barde, Y.A., Duff, K., and Davies, P. (2003). Hyperphosphorylation and aggregation of tau in mice expressing normal human tau isoforms. *J. Neurochem.* *86*, 582–590.
- Andreadis, A. (2005). Tau gene alternative splicing: expression patterns, regulation and modulation of function in normal brain and neurodegenerative diseases. *Biochim. Biophys. Acta* *1739*, 91–103.
- Andreadis, A. (2012). Tau splicing and the intricacies of dementia. *J. Cell. Physiol.* *227*, 1220–1225.
- Andreadis, A., Brown, W.M., and Kosik, K.S. (1992). Structure and novel exons of the human tau gene. *Biochemistry* *31*, 10626–10633.
- Arendt, T., Stieler, J.T., and Holzer, M. (2016). Tau and tauopathies. *Brain Res. Bull.* *126*, 238–292.
- Avale, M.E., Falzone, T.L., Gelman, D.M., Low, M.J., Grandy, D.K., and Rubinstein, M. (2004). The dopamine D4 receptor is essential for hyperactivity and impaired behavioral inhibition in a mouse model of attention deficit/hyperactivity disorder. *Mol. Psychiatry* *9*, 718–726.
- Avale, M.E., Rodríguez-Martín, T., and Gallo, J.M. (2013). Trans-splicing correction of tau isoform imbalance in a mouse model of tau mis-splicing. *Hum. Mol. Genet.* *22*, 2603–2611.
- Bodea, L.-G., Eckert, A., Ittner, L.M., Piguet, O., and Götz, J. (2016). Tau physiology and pathomechanisms in frontotemporal lobar degeneration. *J. Neurochem.* *138* (Suppl 1), 71–94.
- Castillo-Carranza, D.L., Gerson, J.E., Sengupta, U., Guerrero-Muñoz, M.J., Lasagna-Reeves, C.A., and Kaye, R. (2014). Specific targeting of tau oligomers in Htau mice prevents cognitive impairment and tau toxicity following injection with brain-derived tau oligomeric seeds. *J. Alzheimers Dis.* *40* (Suppl 1), S97–S111.
- Castillo-Carranza, D.L., Guerrero-Muñoz, M.J., Sengupta, U., Hernandez, C., Barrett, A.D.T., Dineley, K., and Kaye, R. (2015). Tau immunotherapy modulates both pathological tau and upstream amyloid pathology in an Alzheimer's disease mouse model. *J. Neurosci.* *35*, 4857–4868.
- de Almeida, J., Jourdan, I., Murer, M.G., and Belforte, J.E. (2013). Refinement of neuronal synchronization with gamma oscillations in the medial prefrontal cortex after adolescence. *PLoS ONE* *8*, e62978.
- Duff, K., Knight, H., Refolo, L.M., Sanders, S., Yu, X., Picciano, M., Malester, B., Hutton, M., Adamson, J., Goedert, M., et al. (2000). Characterization of pathology in transgenic mice over-expressing human genomic and cDNA tau transgenes. *Neurobiol. Dis.* *7*, 87–98.
- Goedert, M., Spillantini, M.G., Jakes, R., Rutherford, D., and Crowther, R.A. (1989). Multiple isoforms of human microtubule-associated protein tau: sequences and localization in neurofibrillary tangles of Alzheimer's disease. *Neuron* *3*, 519–526.
- Hutton, M., Lendon, C.L., Rizzu, P., Baker, M., Froelich, S., Houlden, H., Pickering-Brown, S., Chakraverty, S., Isaacs, A., Grover, A., et al. (1998). Association of missense and 5'-splice-site mutations in tau with the inherited dementia FTDP-17. *Nature* *393*, 702–705.
- Lacovich, V., Espindola, S.L., Alloati, M., Pozo Devoto, V., Cromberg, L.E., Čarná, M.E., Forte, G., Gallo, J.-M., Bruno, L., Stokin, G.B., et al. (2017). Tau isoforms imbalance impairs the axonal transport of the amyloid precursor protein in human neurons. *J. Neurosci.* *37*, 58–69.
- Leger, M., Quideville, A., Bouet, V., Haelewyn, B., Boulouard, M., Schumann-Bard, P., and Freret, T. (2013). Object recognition test in mice. *Nat. Protoc.* *8*, 2531–2537.
- Medina, M., Hernández, F., and Avila, J. (2016). New features about tau function and dysfunction. *Biomolecules* *6*, 21.
- Morici, J.F., Bekinschtein, P., and Weisstaub, N.V. (2015). Medial prefrontal cortex role in recognition memory in rodents. *Behav. Brain Res.* *292*, 241–251.
- Morris, M., Maeda, S., Vossel, K., and Mucke, L. (2011). The many faces of tau. *Neuron* *70*, 410–426.
- Niblock, M., and Gallo, J.M. (2012). Tau alternative splicing in familial and sporadic tauopathies. *Biochem. Soc. Trans.* *40*, 677–680.
- Noble, W., Garwood, C., Stephenson, J., Kinsey, A.M., Hanger, D.P., and Anderton, B.H. (2009). Minocycline reduces the development of abnormal tau species in models of Alzheimer's disease. *FASEB J.* *23*, 739–750.
- Paxinos, G., and Franklin, K.B.J. (2011). *The Mouse Brain in Stereotaxic Coordinates* (Academic Press, San Diego).
- Polydoro, M., Acker, C.M., Duff, K., Castillo, P.E., and Davies, P. (2009). Age-dependent impairment of cognitive and synaptic function in the htau mouse model of tau pathology. *J. Neurosci.* *29*, 10741–10749.
- Qian, W., and Liu, F. (2014). Regulation of alternative splicing of tau exon 10. *Neurosci. Bull.* *30*, 367–377.
- Rodríguez-Martín, T., García-Blanco, M.A., Mansfield, S.G., Grover, A.C., Hutton, M., Yu, Q., Zhou, J., Anderton, B.H., and Gallo, J.M. (2005). Reprogramming of tau alternative splicing by spliceosome-mediated RNA trans-splicing: implications for tauopathies. *Proc. Natl. Acad. Sci. U S A* *102*, 15659–15664.
- Rodríguez-Martín, T., Anthony, K., García-Blanco, M.A., Mansfield, S.G., Anderton, B.H., and Gallo, J.M. (2009). Correction of tau mis-splicing caused by FTDP-17 MAPT mutations by spliceosome-mediated RNA trans-splicing. *Hum. Mol. Genet.* *18*, 3266–3273.
- Schoch, K.M., DeVos, S.L., Miller, R.L., Chun, S.J., Norrbom, M., Wozniak, D.F., Dawson, H.N., Bennett, C.F., Rigo, F., and Miller, T.M. (2016). Increased 4R-tau induces pathological changes in a human-tau mouse model. *Neuron* *90*, 941–947.
- Spillantini, M.G., and Goedert, M. (2013). Tau pathology and neurodegeneration. *Lancet Neurol.* *12*, 609–622.
- Spillantini, M.G., Murrell, J.R., Goedert, M., Farlow, M.R., Klug, A., and Ghetti, B. (1998). Mutation in the tau gene in familial multiple system tauopathy with presenile dementia. *Proc. Natl. Acad. Sci. U S A* *95*, 7737–7741.
- Stanford, P.M., Shepherd, C.E., Halliday, G.M., Brooks, W.S., Schofield, P.W., Brodaty, H., Martins, R.N., Kwok, J.B.J., and Schofield, P.R. (2003). Mutations in the tau gene that cause an increase in three repeat tau and frontotemporal dementia. *Brain* *126*, 814–826.